Proceedings of the 28th IEEE
EMBS Annual International Conference
New York City, USA, Aug 30-Sept 3, 2006

Analysis of Capacitive Coupling within Microelectrode Array

Z. Hu, P. R. Troyk, D. E. Detlefsen

***Abstract*—Capacitive coupling within high-density microelectrode arrays can degrade neural recording signal or disperse neural stimulation current. Material deterioration in a chronically implanted neural stimulation/recording system can cause such an undesired effect. We present a simple method with an iterative algorithm to quantify the cross-coupling capacitance, *in-situ*.**

I. Introduction

MULTIPLE-electrode arrays (MEA), with both surface and penetrating microelectrodes, are widely used many types of neural stimulation/recording applications. Several common features of the design of MEAs [1], [2] include: close spacing (on the order of 100 μm) of the microelectrodes; electrodes are welded onto an substrate in the array form; a multi-thread flexible cable that connects the substrate to some form of a percutaneous connector, which then interfaces with the external stimulating/recording electronics. Capacitive coupling of electrical signals between isolated microelectrodes exists at all these stages (Fig. 1), and should be minimized for proper functioning of the system. However, when the MEA is implanted *in-vivo* or is used chronically, deterioration of insulating materials, such as may be caused by water saturation of a polymer at the connector, on the substrate, or in the cable, may increase the dielectric constant and thus increase the coupling capacitance among the microelectrodes. This in effect converts the multiple small electrodes in an array into a "large" electrode, which looses neural selectivity in electrical stimulation and degrades amplitude of the neural signal in neural recording.

In this paper, we present a simple method that uses the custom-designed compliance-limited neural stimulation chip to automatically estimate the coupling capacitance among a large number of microelectrodes in an implanted MEA system.

II. Method

A. Hardware

Our compliance-limited neural-stimulation chip was originally designed and optimized for driving AIROF microelectrodes (see companion paper EMBC06). Each single chip is capable of driving 16 AIROF microelectrodes in one array simultaneously. To achieve high charge delivery capacity, the electrodes were D.C. coupled and anodically biased [3]. To protect the electrode from irreversible damage, the chip also uses a compliance-limited driving strategy [4] that basically clamps the electrode voltage within ±0.6 V vs. a Ag/AgCl reference electrode. As shown in Fig. 2, there are two current sources for each channel. One provides the anodic current and thus anodically biases the electrode during the interpulse interval. The other provides cathodic current for neural stimulation.

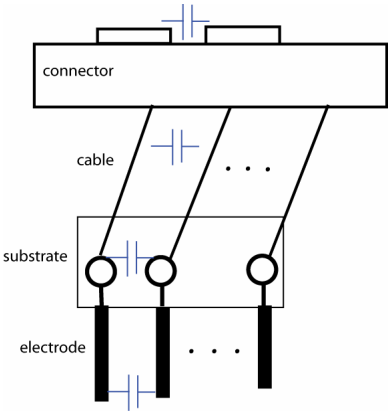

Fig. 1. Possible locations of undesired capacitive coupling within microelectrode array system.

This same system can help us estimate the coupling capacitor among microelectrodes in one array as we configure the chip to use a monophasic, cathodic-first current pulse stimulation mode. For monitoring the voltage and current conditions for each electrode, there is one voltage monitor circuit built on the chip that can be

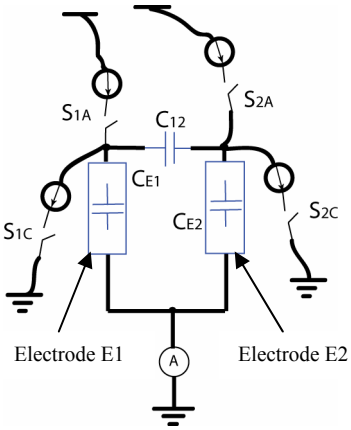

Fig. 2. Diagram of our stimulation chip connected to two electrodes E1 and E2, characterized by capacitors C_{E1} and C_{E2}, with a coupling capacitor C_{12} between them.

Z. Hu is with the Biomedical Engineering Department, Illinois Institute of Technology, Chicago, IL 60616 USA

P. R. Troyk is with the Biomedical Engineering Department, Illinois Institute of Technology, Chicago, IL 60616 USA

D. E. Detlefsen is with the Biomedical Engineering Department, Illinois Institute of Technology, Chicago, IL 60616 USA.

multiplexed to measure voltage of each electrode, and there is one current monitor circuit in series with the counter electrode to measure the total return current.

B. Experiment Procedure (Simple Case)

Start with the simplest case of capacitive coupling between two electrodes E1 and E2, as shown in Fig. 2. Since we are interested in estimating the coupling capacitor C_{12}, we can simplify the electrode impedance to be a simple capacitor as well (C_{E1} and C_{E2}).

(a) First, we drive electrode E1 so that its voltage reaches the cathodic compliance limit while leaving E2 disconnected, i.e. S_{1C} closed and S_{1A}, S_{2A}, S_{2C} open, the return current measured at the counter electrode can be used to compute the total charge delivered Q_a through both the electrode C_{E1} and the branch of electrode C_{E2} in series with the coupling capacitor C_{12}.

The effect of C_{12} is undesirable. In the case of neural stimulation, the stimulation current will be distributed between electrodes E1 and E2. In the case of neural recording, the neural signal being picked up at the electrode site E1 will be loaded down by E2 and interfered with by signal from the electrode site E2.

(b) Secondly, we once again drive the electrode E1 to the cathodic compliance limit, as before, but this time with electrode E2 biased, i.e. S_{1C}, S_{2A} close and S_{1A}, S_{2C} open; the voltage of E2 is now held at the anodic bias point. In this case, by measuring the return current at the counter electrode the charge Q_b delivered only through electrode E1, can be computed.

Assuming the charge delivered on E1 in both steps (a), (b) is the same, owing to maintaining the same voltage excursion, the difference Q_a–Q_b is the charge being delivered through the extra capacitor in the branch of electrode C_{E2} in series with the coupling capacitor C_{12}. This difference can then be used to calculate C_{12}.

C. Analysis

The equivalent circuits for step (a) and step (b) are shown in Fig. 3.

The following set of equations describes both of these circuits and introduces k_{12} and k_{21} which can be used in (3) to compute C_{12}.

$$\begin{cases} Q_a = Q_1 + Q_2 \\ Q_b = Q_1 \\ Q_1 = C_1 \cdot V \\ Q_2 = \dfrac{C_2 \cdot C_{12}}{C_{12} + C_2} \cdot V \end{cases} \Rightarrow \frac{Q_1}{Q_2} = k_{12} = \frac{C_1}{\dfrac{C_2 \cdot C_{12}}{C_{12} + C_2}} \quad (1)$$

k_{12} can be determined by applying the experimental procedure on electrode E1. As we perform the same procedure on electrode E2, k_{21} can be similarly calculated:

$$k_{21} = \frac{C_2}{\dfrac{C_1 \cdot C_{12}}{C_{12} + C_1}} \quad (2)$$

Solving equation (1) and (2) gives the coupling capacitor C_{12} in relation to C_1 and C_2.

$$C_{12} = \frac{(1+k_{12})C_2}{k_{12}k_{21} - 1} = \frac{(1+k_{21})C_1}{k_{12}k_{21} - 1} \quad (3)$$

D. Extended to Array of 16 Microelectrodes or More

In an array of 16 microelectrodes, a microelectrode E1 could have coupling capacitors with the other 15 electrodes. This is the case for all electrodes E2, E3, ..., E16. Therefore, there are a total of 120 possible coupling capacitors among 16 electrodes. The procedure described above can be extended to estimating all these coupling capacitors.

In an array of 16 electrodes, in the worst case, each electrode can be coupled to the other 15 ones.

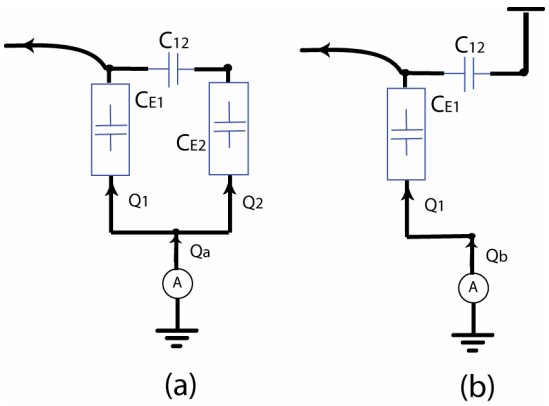

Fig. 3. Equivalent circuits for step (a) and step (b).

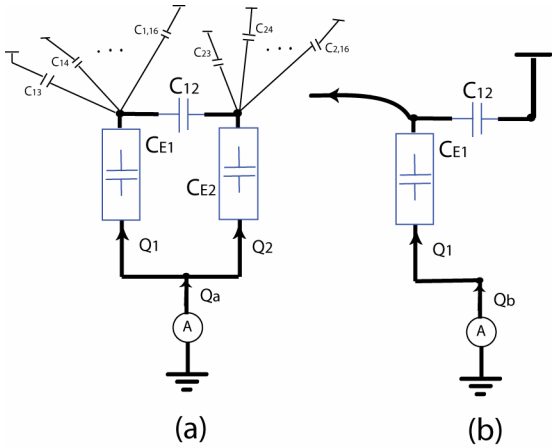

Fig. 4. Equivalent circuits for step (a) and step (b).

As shown in Fig. 4, when we bias all the other 14 electrodes, but leave E2 disconnected, as in step (a), the extra capacitor that causes a charge difference between step (a) and step (b) is not merely C_{12} in series with C_2. Because the rest of the coupling capacitors connected to the electrode E2, are in parallel ($\sum C_{2i}$), they will also source current into C_{12}, and the equivalent capacitor becomes:

$$\frac{1}{C_{eq}} = \frac{1}{C_2} + \frac{1}{\frac{C_2}{C_2 + \sum_j C_{2j}} \cdot C_{12}} \quad (4)$$

in which C_{12} is scaled down by $\frac{C_2}{C_2 + \sum_j C_{2j}}$ (5)

So if we still use the earlier formula (3) to estimate C_{12}, it will be under-estimated. In order to correctly estimate the 120 coupling capacitors C_{ij} in an array, we introduce two new parameters t_1 and t_2:

$$\begin{cases} t_1 \cdot C_1 = C_1 + \sum_i C_{1i} \\ t_2 \cdot C_2 = C_2 + \sum_i C_{2i} \end{cases} \quad (6)$$

The modified formula for estimating C_{12} becomes:

$$C_{12} = \frac{(t_2 + k_{12}t_1)C_2}{k_{12}k_{21} - 1} = \frac{(t_1 + k_{21}t_2)C_1}{k_{12}k_{21} - 1} \quad (7)$$

In formula (7), k_{12} and k_{21} come directly from the earlier experimental procedure, and t_1 and t_2 set the linear relationship between C_{12} and the other coupling capacitors. Through our experimental measurements, we will have 120 independent linear system equations $A\,x = b$ to solve for determining the 120 coupling capacitors C_{ij}. Equation (7) essentially provides a recursive formula to iteratively solve the linear equations.

$$x^{(k+1)} = B\,x^{(k)} + c$$

Mathematically the sufficient and necessary condition for the iterative method to converge is that the spectrum radius of matrix **B** is less than 1.

A convergence check on matrix **B** can be performed at the onset, though errors in the measurements or certain conditions, such as a short-circuit between two electrodes, making the coupling capacitor between them approach infinity, may cause the algorithm to fail. One advantage of this iterative algorithm is that one can heuristically leave out undesirable coupling capacitor values C_{qr} in the summation of formula (6) such that the algorithm can converge. By doing so, we basically segment the coupling problem into smaller groups, which results in underestimating some of coupling capacitors and the estimation errors in many cases are acceptable.

E. Extended Experiment Procedure for Coupling between 16 Electrodes

A practical experimental procedure to enable estimation of 120 coupling capacitor more accurately (Fig. 4.) becomes:

(a) Drive electrode E1 to the cathodic limit; leave E2 disconnected and bias all the other 14 electrodes. Measure Q_a.

(b) Drive the electrode E1 to the cathodic limit and bias the remaining 15 electrodes, (including E2). Measure Q_b.

(c) k_{12} can be calculated by $Q_b/(Q_a\text{-}Q_b)$

(d) Move on to electrode E2 and do the steps (a) and (b) with E1↔E2 switched. k_{21} can then be calculated.

(e) Pick another pair of electrodes E_i and E_j. For each pair a new set of k_{ij} and k_{ji} can be calculated from the charge measurement by the previous steps.

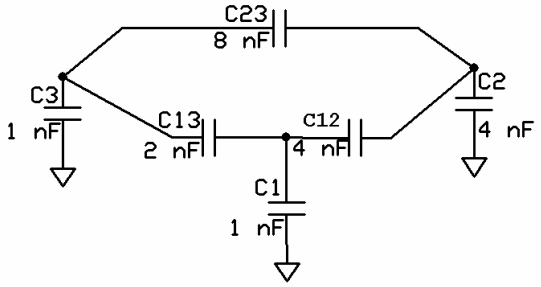

Fig. 5. Demonstration circuit of three electrodes with coupling capacitor in between.

For an array of 16 electrodes, our custom LabView program can picks 120 pairs sequentially and make altogether 256 measurements within 5 minutes.

III. DEMONSTRATION

As a demonstration, suppose we have a capacitor network of three nodes representing three electrodes E_1, E_2, E_3 and the coupling capacitor between them, as shown in Fig. 5.

Following the charge measuring procedure in the previous section, the six k-values can be calculated:

$$\begin{cases} k_{12} = 1 \\ k_{21} = 7 \end{cases} \quad \begin{cases} k_{23} = 5.5 \\ k_{32} = 0.5 \end{cases} \quad \begin{cases} k_{13} = 5.5 \\ k_{31} = 3.5 \end{cases}$$

Knowing these k-values and the electrode capacitor C_1, C_2, and C_3, the three coupling capacitors can be calculated by the iterative code in Mathematica:

```
c12[{c12_, c23_, c13_}] := With[{t1 = c13/c1 + 1, t2 = c23/c2 + 1},
  (k12 t1 + t2) c2/(k12 k21 - 1) /. {k12 → 1, k21 → 7, c1 → 1, c2 → 4, c3 → 1}]
c23[{c12_, c23_, c13_}] := With[{t1 = c12/c2 + 1, t2 = c13/c3 + 1},
  (k23 t1 + t2) c3/(k23 k32 - 1) /. {k23 → 5.5, k32 → 0.5, c1 → 1, c2 → 4, c3 → 1}]
c13[{c12_, c23_, c13_}] := With[{t1 = c12/c1 + 1, t2 = c23/c3 + 1},
  (k13 t1 + t2) c3/(k13 k31 - 1) /. {k13 → 5.5, k31 → 3.5, c1 → 1, c2 → 4, c3 → 1}]
FixedPoint[Through[{c12, c23, c13}[#1]] &, {0.1, 0.1, 0.1}, 50]
```

```
{4., 8., 2.}
```

In this case (Fig. 6), the convergence is guaranteed since the eignvalues of the matrix **B** are: $\{0.67, -0.50, -0.17\}$, and their absolute values are

all less than 1. Starting with an initial guess of 0.1 for each coupling capacitor, after 37 steps of iteration, the algorithm reached asymptotes for the correct coupling capacitor values $C_{12} = 4$; $C_{23} = 8$, and $C_{13} = 2$ as the fixed-point of the iterations.

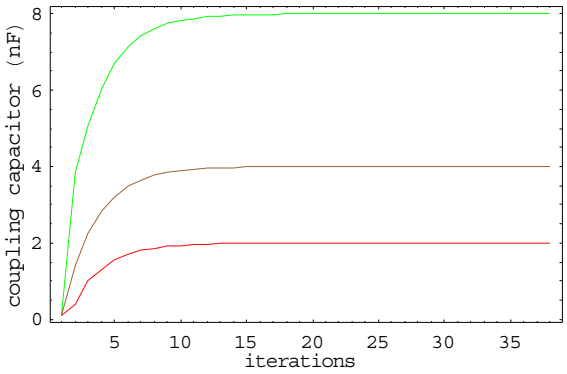

Fig. 6. Demonstration circuit of three electrodes with coupling capacitor in between.

IV. Conclusion & Discussion

In our visual prosthesis research project, six 16-electroode MEAs were implanted in the visual cortex of a male Macaque monkey. As we keep on monitoring the charge capacity of these electrodes [5], some of the electrodes in the array show increasing charge capacity and the neural recording signal from these electrodes becomes weaker. All these seem to be the evidence of capacitive coupling between the electrodes in the array and we suspect that these increasing coupling capacitors are due to the material deterioration in the cables that lead the array into the head connector. We are planning to perform a comprehensive coupling capacitor diagnosis experiment.

Equipped with our neural stimulation chip system and this coupling capacitor estimation algorithm, we can quickly evaluate and routinely check the capacitive coupling effect in situ. It can be very important for monitoring the long-term stability of such chronically implanted MEA systems.

References

[1] D. McCreery, A. Lossinsky, V. Pikov, and X. Liu, "Microelectrode array for chronic deep-brain microstimulation and recording," IEEE Trans Biomed Eng, vol. 53, pp. 726-37, 2006.

[2] J. Kitzmiller, D. Beversdorf, and D. Hansford, "Fabrication and testing of microelectrodes for small-field cortical surface recordings," Biomed Microdevices, vol. 8, pp. 81-5, 2006.

[3] X. Beebe and T. L. Rose, "Charge Injection Limits of Activated Iridium Oxide Electrodes with 0.2 ms Pulses in Bicarbonate Buffered Saline," IEEE Transactions on Biomedical Engineering, vol. 35, pp. 494-495, 1988.

[4] N. R. Srivastava, P. R. Troyk, and S. F. Cogan, "A laboratory testing and driving system for AIROF microelectrodes," presented at Engineering in Medicine and Biology Society, 2004. EMBC 2004. Conference Proceedings. 26th Annual International Conference of the, 2004.

[5] Z. Hu, P. R. Troyk, and S. F. Cogan, "Comprehensive Cyclic Voltammetry Characterization of AIROF Microelectrodes," presented at Engineering in Medicine and Biology Society, 2005. IEEE-EMBS 2005. 27th Annual International Conference of the, 2005.